Formal Worst-Case Analysis of Crosstalk Noise in Mesh-Based Optical Networks-on-Chip

Yiyuan Xie, Mahdi Nikdast, *Student Member, IEEE*, Jiang Xu, *Member, IEEE*, Xiaowen Wu, *Student Member, IEEE*, Wei Zhang, *Member, IEEE*, Yaoyao Ye, *Student Member, IEEE*, Xuan Wang, *Student Member, IEEE*, Zhehui Wang, *Student Member, IEEE*, and Weichen Liu, *Member, IEEE*

***Abstract*— Crosstalk noise is an intrinsic characteristic as well as a potential issue of photonic devices. In large scale optical networks-on-chips (ONoCs), crosstalk noise could cause severe performance degradation and prevent ONoC from communicating properly. The novel contribution of this paper is the systematical modeling and analysis of the crosstalk noise and the signal-to-noise ratio (SNR) of optical routers and mesh-based ONoCs using a formal method. Formal analytical models for the worst-case crosstalk noise and minimum SNR in mesh-based ONoCs are presented. The crosstalk analysis is performed at device, router, and network levels. A general 5 × 5 optical router model is proposed for router level analysis. The minimum SNR optical link candidates, which constrain the scalability of mesh-based ONoCs, are identified. It is also shown that symmetric mesh-based ONoCs have the best SNR performance. The presented formal analyses can be easily applied to other optical routers and mesh-based ONoCs. Finally, we present case studies of mesh-based ONoCs using the optimized crossbar and Crux optical routers to evaluate the proposed formal method. We find that crosstalk noise can significantly limit the scalability of mesh-based ONoCs. For example, when the mesh-based ONoC size, using optimized crossbar, is larger than 8 × 8, the optical signal power is smaller than the crosstalk noise power; when the network size is 16 × 16 and the input power is 0 dBm, in the worst-case, the signal power is −24.9 dBm and the crosstalk noise power is −11 dBm.**

***Index Terms*— Optical crosstalk noise, optical losses, optical networks-on-chip, signal-to-noise ratio.**

I. Introduction

With the increase in the number of integrated processing cores on a single die, processor data rate will quickly reach several tens of GHz, which results in larger bandwidth requirement, higher intra/inter-chip transmission time, and higher power consumption [1]. As scaling helps transistors to become faster and less power hungry, interconnects are not able to keep pace with the performance of the transistors, thereby creating a performance bottleneck. Switched on-chip global networks have been proposed as an attractive solution to mitigate the emerging communication bottlenecks appear in the current generation of electronic cross-chip point-to-point interconnects [2]. The International Technology Roadmap for Semiconductors predicts that interconnects will become the most critical issue in the near future [3].

Optical networks-on-chips (ONoCs) are based on photonic technology and use silicon-based optical interconnects and routers, which are compatible with CMOS technology [4]. Recently, studies have highlighted some advantages of ONoCs, including great potentials to achieve significantly higher bandwidth, lower power dissipation, and lower latency in comparison with electronic NoCs [5].

Several optical on-chip communication architectures and optical routers have been proposed based on optical waveguides and microresonators. Silicon waveguide crossing and microresonator-based photonic switching elements are extensively used in ONoCs. A major shortcoming of the crossing and microresonator-based switching is crosstalk. Crosstalk is the result of undesirable coupling between optical signals. Reference [6] indicated that the waveguide crossings play an essential role in the network performance degradation. Some efforts have been made to reduce the crosstalk noise and power loss in waveguide crossings. Sanchis *et al.* [7] offered the method of choosing the optimum crossing angle to reduce the crosstalk noise. Bogaerts *et al.* [8] proposed a design uses parabolically broadened waveguides and a double etch scheme to reduce lateral refractive index contrast while still confining the light as much as possible in the crossing region. Chen *et al.* [9] proposed multimode-interference (MMI)-based wire waveguide crossings, instead of conventional plain waveguide crossings, for the merits of low loss and low crosstalk. Chen *et al.* [10] presented a design technique for a compact 5426 × 5426 nm waveguide crossing by using a 90° MMI-based waveguide crossing sandwiched by four identical miniaturized and improved the insertion loss and the crosstalk noise to −0.21 dB and −44.4 dB at the wavelength of 1550 nm. Li *et al.* [11] demonstrated metal-free integrated elliptical reflectors for waveguide turnings and crossings. By employing four symmetric identical elliptical reflectors sharing an intermediate beam focused region in direct waveguide crossing, the crosstalk noise smaller than −30 dB,

Manuscript received July 10, 2011; revised July 12, 2012; accepted August 31, 2012. Date of publication November 16, 2012; date of current version September 9, 2013. This work was supported in part by HKUST PDF, SBI06/07. EG01-4, and RPC11EG18 of the Hong Kong SAR, China. The work of Y. Xie was supported by the Post-Doctoral Fund from Hong Kong University of Science and Technology.

Y. Xie, M. Nikdast, J. Xu, X. Wu, Y. Ye, X. Wang, Z. Wang, and W. Liu are with the Department of Electronic and Computer Engineering, Hong Kong University of Science and Technology, Hong Kong (e-mail: jiang.xu@ust.hk).

W. Zhang is with the School of Computer Engineering, Nanyang Technological University, 637820, Singapore.

Color versions of one or more of the figures in this paper are available online at http://ieeexplore.ieee.org.

Digital Object Identifier 10.1109/TVLSI.2012.2220573

and high transmission were achieved. An ultracompact waveguide crossing with negligible crosstalk noise and insertion loss was proposed in [12] in which the waveguide cross is field with impedance matched metamaterial, which effectively suppresses the diffraction of the guided mode in the crossing region.

The crosstalk noise and signal-to-noise ratio (SNR) of the mesh-based ONoCs using the optimized optical crossbar router were analyzed in [6]. Moreover, a novel compact high-SNR optical router, called Crux, was proposed to improve the scalability of ONoCs. In this paper, the method used in [6] is developed and generalized to enable the crosstalk noise and SNR analyses in the mesh-based ONoCs using arbitrary 5×5 optical router. In [13], a methodology to characterize and model basic photonic blocks, which can form full photonic network architectures, was presented. Reference [14] proposed a hybrid global router, called GLOW, to provide low power interconnects considering the thermal reliability and physical design constraints. Reference [15] indicated that the crosstalk noise is an intrinsic, serious issue in directional-coupler-based optical networks. Reference [16] developed a modeling methodology that describes the optical and electrical behaviors of silicon photonic devices.

Crosstalk noise is of critical concern to multihop ONoCs, such as mesh-based ONoCs. For the first time, this paper proposes the systematical analysis of the worst-case crosstalk noise and SNR for the mesh-based ONoCs at device, router, and network levels. The analytical models for the worst-case crosstalk noise and SNR are proposed. Different longest optical links in the mesh-based ONoCs are analyzed and their SNR are modeled to find the minimum SNR link in the network. All of the analyses are based on a general 5×5 optical router model presented in this paper. The general optical router model can be applied to any other 5×5 optical routers. The case studies of mesh-based ONoCs using optimized crossbar and Crux optical routers are presented to validate our proposed method. The conclusions drawn in this paper can indicate how promising mesh-based ONoCs are among other possible ONoCs architectures. The proposed systematical formal model does not take into account dynamic variations of optical devices, such as the laser noise and thermal noise.

The rest of this paper is organized as follows. Basic optical switching elements (BOSEs) and the general optical router model are described in Section II. Section III includes the network level analysis to find the minimum SNR link. In Section IV, the SNR of the minimum SNR link candidates in mesh-based ONoCs is numerically simulated and compared. The mesh-based ONoCs using optimized crossbar and Crux optical routers evaluate the proposed analytical models in Section V. Finally, we draw conclusions in Section VI.

II. BOSEs and General Optical Router Model

Mesh-based ONoC consists of functional cores and optical routers that are connected to each other by channels through the mesh topology. Each router is connected to four neighboring routers via input and output channels. The mesh-based ONoC is a hybrid structure, and consists of two overlapped networks with the same topology. First, an electronic network is used for routing control packets based on packet switching and also controlling optical network. Second, optical network is responsible for routing payload packets using circuit switching. The optical data network and the electronic control network can be implemented in different layers. The optical and metallic interconnects are all bidirectional. The architecture can be fabricated using 3-D IC technologies.

The optical router is the key component in building different types of ONoCs. Its function is to establish and maintain optical paths from the source to the destination for an optical signal, which carries payload data. On the one hand, the physical limitations imposed by integration necessitate a compact and low loss design while maintaining the maximum level of functionality. On the other hand, although these two requirements are important, the minimum crosstalk noise is essential since the basic function of ONoC is to faultlessly transmit information. This section covers device and router levels analyses.

A. Basic Optical Elements

In the construction of integrated optical circuits, space restrictions and the desire to operate on multiple input waveguides necessitate waveguide crossings. Without low-loss and low-crosstalk waveguide crossings, routing of complex photonic circuits is difficult or even impossible [8]. In most of the crossings used in ONoCs, the latitudinal and longitudinal waveguides are in the same plane. In a perfect crossing arrangement, optical modes propagate with 100% transmission from an input waveguide to an output one on the opposite side of the crossing intersection, with no reflection and with 0% transmission (crosstalk) to the other outputs. However, the ideal crossing is impossible due to the coupling of the four branches, or ports, of the intersection in terms of a resonant cavity at the center. If resonant modes that are excited from the input port could be prevented by symmetry from decaying into the transverse ports, then the crosstalk noise would be eliminated. Nevertheless, the perfect crossing could not be attained.

Waveguides and microresonators form different types of BOSEs, which are the key components in optical routers. Optical routers consist of BOSEs, waveguide crossings, waveguides, and optical terminators. Two types of basic 1×2 optical switching elements are the parallel switching element (PSE) and the crossing switching element (CSE). The PSE is built from a microresonator located between two parallel waveguides as shown in Fig. 1(b) and (c). The structure consists of a microresonator adjacently positioned next to a waveguide intersection is called CSE (Fig. 2). Microresonators have a certain resonance frequency, derived from the material and structural properties. Basic optical switching elements can be powered on (ON state) or off (OFF state) according to the following.

1) OFF state: The wavelength (λ_S) of the optical signal is different from the resonant frequency of the ring (λ_{off}). The input optical signal propagates from the input port

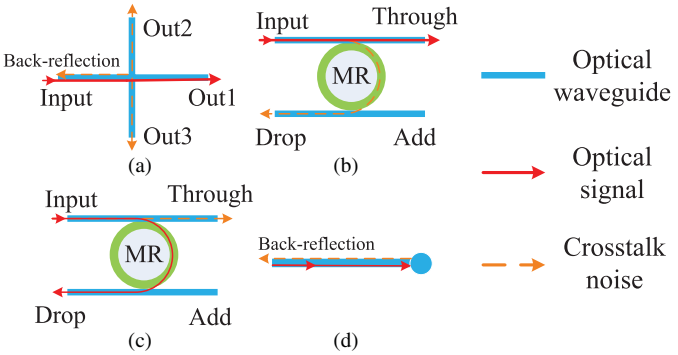

Fig. 1. (a) Waveguide crossing. (b) PSE in OFF state. (c) PSE in ON state. (d) Optical terminator.

TABLE I

NOTATIONS FOR LOSSES, CROSSTALK, AND REFLECTANCE COEFFICIENTS

Parameter	Notation
Crossing loss	L_c
Propagation loss per cm	L_p
Power loss per CSE in OFF state	$L_{c,\text{off}}$
Power loss per CSE in ON state	$L_{c,\text{on}}$
Bending loss	L_b
Power loss per PSE in OFF state	$L_{p,\text{off}}$
Power loss per PSE in ON state	$L_{p,\text{on}}$
Crossing's crosstalk coefficient	K_c
Crosstalk coefficient per PSE in OFF state	$K_{p,\text{off}}$
Crosstalk coefficient per PSE in ON state	$K_{p,\text{on}}$
Crossing's back-reflection coefficient	K_r
Optical terminator's reflectance coefficient	K_t

to the through port when the microresonator is powered off [Figs. 1(b) and 2(a)].

2) ON state: The switch is turned on by injecting an electrical current into the p-n contacts surrounding the ring or changing the temperature using the metal-plate based thermal heating. The resonance frequency (λ_{on}) of the microresonator shifts so that the light ($\lambda_S = \lambda_{\text{on}}$), now on resonance, is coupled into the ring and directed to the drop port, thus causes a switching action [Figs. 1(c) and 2(b)].

The waveguide crossing as shown in Fig. 1(a) has an input port and three possible output ports- out1, out2, and out3. When two optical signals go through a crossing simultaneously, crosstalk will be created at the crossing. Moreover, the small portion of light will reflect back on the input port. Given P_{in} as the input optical power, the output powers at out1, out2, and out3 ports as a function of P_{in} are calculated in (1). In this paper, Table I helps to understand the notations used in the equations. In the following equations, P_{out1}, P_{out2}, and P_{out3} are the output powers at out1, out2, and out3, respectively, and P_{Rc} is the reflected power on the input port:

$$P_{\text{out1}} = L_c P_{\text{in}} \tag{1a}$$
$$P_{\text{out2}} = P_{\text{out3}} = K_c P_{\text{in}} \tag{1b}$$
$$P_{Rc} = K_r P_{\text{in}}. \tag{1c}$$

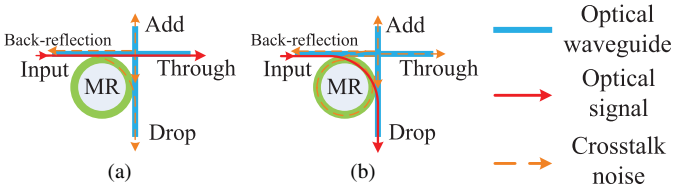

Fig. 2. CSE. (a) OFF state. (b) ON state.

The PSE can be either in OFF or ON state [Fig. 1(b) and (c)]. The output powers at the through port (P_T) and drop port (P_D) as a function of input optical power are calculated based on (2) for the OFF state and (3) for the ON state. In this paper, the negligible crosstalk noise on the add port of the PSE is not considered

$$P_{T\,\text{pse,off}} = L_{p,\text{off}} P_{\text{in}} \tag{2a}$$
$$P_{D\,\text{pse,off}} = K_{p,\text{off}} P_{\text{in}} \tag{2b}$$
$$P_{D\,\text{pse,on}} = L_{p,\text{on}} P_{\text{in}} \tag{3a}$$
$$P_{T\,\text{pse,on}} = K_{p,\text{on}} P_{\text{in}} \tag{3b}$$
$$P_{Rt} = K_t P_{\text{in}}. \tag{4}$$

The basic function of the optical terminators, Fig. 1(d), is to avoid the light from reflecting back on the input port. The reflected power, P_{Rt}, of the optical terminator can be written as (4).

Compared with the PSE, the CSE has a waveguide crossing that introduces nonnegligible crossing insertion loss. When the CSE is in OFF state [see Fig. 2(a)], the output powers at different ports are calculated based on (5) and when it is in ON state [see Fig. 2(b)], (6) calculates the output powers. P_A is the output power at the add port and P_{Rcse} indicates the reflected power on the input port of CSE

$$P_{T\,\text{cse,off}} = L_{c,\text{off}} P_{\text{in}} \tag{5a}$$
$$P_{D\,\text{cse,off}} = (K_{p,\text{off}} + L_{p,\text{off}}^2 K_c) P_{\text{in}} \tag{5b}$$
$$P_{A\,\text{cse,off}} = K_c L_{p,\text{off}} P_{\text{in}} \tag{5c}$$
$$P_{R\,\text{cse,off}} = K_r L_{p,\text{off}}^2 P_{\text{in}} \tag{5d}$$
$$P_{D\,\text{cse,on}} = L_{c,\text{on}} P_{\text{in}} \tag{6a}$$
$$P_{T\,\text{cse,on}} = K_{p,\text{on}} P_{\text{in}} (L_c(1 + K_c L_{p,\text{on}}) + K_r L_{p,\text{on}} K_c) \tag{6b}$$
$$P_{A\,\text{cse,on}} = K_{p,\text{on}} P_{\text{in}} (K_c(1 + K_c L_{p,\text{on}}) + K_r L_{p,\text{on}} L_c) \tag{6c}$$
$$P_{R\,\text{cse,on}} = K_{p,\text{on}} K_r P_{\text{in}}. \tag{6d}$$

According to Fig. 2(a), when the CSE is in OFF state, the power loss, $L_{c,\text{off}}$, can be calculated based on the models of waveguide crossing and PSE in OFF state which results in $L_c L_{p,\text{off}}$. Moreover, for the ON state, as shown in Fig. 2(b), the power loss, $L_{c,\text{on}}$, can be calculated by using the models of PSE in ON state and the waveguide crossing which results in $L_{p,\text{on}}(1 + K_{p,\text{off}} K_c^2) + K_{p,\text{on}}^2 K_c$. Considering the latter equation, since crosstalk coefficients are very small numbers ($K_i K_j \cong 0$), $L_{c,\text{on}}$ can be approximated by $L_{p,\text{on}}$.

B. General Optical Router Model

The general optical router model is proposed to analyze the crosstalk noise and SNR at the router level and later at

the network level for the mesh-based ONoCs. The proposed general model, as shown in Fig. 3, is based on a 5×5 optical router and follows dimension-order routing algorithm. It has five input and five output ports including: Injection/Ejection, North, East, South, and West. Each port is defined as I_i^j where the subscript i defines the port number. The value of i for different ports varies from 0 to 4 according to: $i = 0$ for the Injection/Ejection port, $i = 1$ for the North port, $i = 2$ for the East port, $i = 3$ for the South port, and $i = 4$ for the West port. Moreover, $j = 0$ shows that the port is an input one and $j = 1$ indicates that the port is an output one. The general model can be applied to other 5×5 optical routers.

$L_{i,j}(x, y)$, defined in (7a), is the insertion loss from the ith port to the jth port in the router $R(x, y)$. In this equation, $L_{i,j}^{OR}(x, y)$, as shown in (7b), indicates the power loss introduced by the optical router $R(x, y)$. It includes the switching power loss, $S_{Li,j}(x, y)$, caused by the switching elements and waveguide crossings, and the propagation loss inside the optical router, which is calculated by considering the waveguide length between the ith input port and the jth output port, $W_{li,j}(x, y)$, and the propagation loss, L_p. We integrate the propagation loss at the network level into our general optical router model; when the output port is not Ejection, $j \neq 0$, we consider the propagation loss of the waveguide connects the optical router $R(x, y)$ to the next optical router as shown in (7a). D is the hop-length and can be calculated based on (7c) for the homogeneous symmetrical ONoCs. S is the chip size (cm^2) and $M \times N$ is the network size

$$L_{i,j}(x, y) = \begin{cases} L_{i,0}^{OR}(x, y), & j = 0 \\ L_{i,j}^{OR}(x, y) L_p^D, & j \neq 0 \end{cases} \tag{7a}$$

$$L_{i,j}^{OR}(x, y) = S_{Li,j}(x, y) L_p^{W_{li,j}(x,y)} \tag{7b}$$

$$D \cong \sqrt{\frac{S}{M \times N}} \tag{7c}$$

$$i, j \in \{0, \ldots, 4\}, \quad x \in \{1, \ldots, M\}, \quad y \in \{1, \ldots, N\}.$$

$s_{i,j}(x, y)$ is the status of the router $R(x, y)$ while an optical signal is traveling from the ith port to the jth port. The router status is defined in (8) according to the dimension-order routing algorithm. In this equation, I_a^0, I_b^0, I_c^0, I_d^0, and I_e^0 are the input ports associated with the output ports I_0^1, I_1^1, I_2^1, I_3^1, and I_4^1, respectively. Moreover, -1 is used when the output port is free. For example, $s_{0,2}(x, y)(I_{-1}^0, I_3^0, I_0^0, I_{-1}^0, I_{-1}^0)$ indicates that there is an optical signal traveling from the south port to the north port, $b = 3$, in the router $R(x, y)$ while there is no signal exists at the ejection, south output, and west output ports, $a = d = e = -1$, and the main optical signal is traveling from the injection port toward the east port, $i = 0, j = 2$, and $c = 0$

$$s_{i,j}(x, y) = (I_a^0, I_b^0, I_c^0, I_d^0, I_e^0) \begin{matrix} a \in \{-1, 1, 2, 3, 4\} \\ b \in \{-1, 0, 2, 3, 4\} \\ c \in \{-1, 0, 4\} \\ d \in \{-1, 0, 1, 2, 4\} \\ e \in \{-1, 0, 2\}. \end{matrix} \tag{8}$$

$P_{i,j}(x, y)$, calculated in (9), is defined as the optical power outputted by the jth port caused by the optical power, $P_i^0(x, y)$, injected into the ith port in the router $R(x, y)$

$$P_{i,j}(x, y) = P_i^0(x, y) L_{i,j}(x, y)$$
$$i, j \in \{0, \ldots, 4\}, \quad x \in \{1, \ldots, M\}, \quad y \in \{1, \ldots, N\}. \tag{9}$$

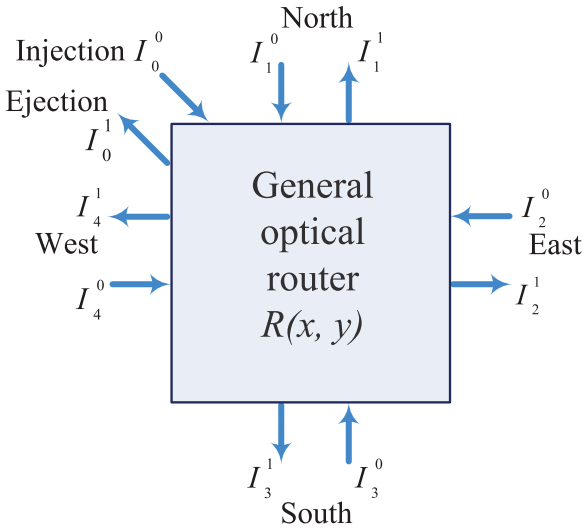

Fig. 3. General 5×5 optical router model.

$N_{i,j}(x, y, s_{i,j}(x, y))$, calculated in (10), is defined as the crosstalk noise added to the optical signal traveling from the ith port to the jth port, and $K_{i,j,m}(s_{i,j}(x, y))$ is defined as the crosstalk noise coefficient introduced by $P_m^0(x, y)$ to the optical signal in the router $R(x, y)$ under the status s

$$\begin{aligned} N_{i,j}(x, y, s_{i,j}(x, y)) = {} & P_0^0(x, y) K_{i,j,0}(s_{i,j}(x, y)) \\ & + P_1^0(x, y) K_{i,j,1}(s_{i,j}(x, y)) \\ & + P_2^0(x, y) K_{i,j,2}(s_{i,j}(x, y)) \\ & + P_3^0(x, y) K_{i,j,3}(s_{i,j}(x, y)) \\ & + P_4^0(x, y) K_{i,j,4}(s_{i,j}(x, y)) \end{aligned}$$
$$i, j \in \{0, \ldots, 4\}, \quad x \in \{1, \ldots, M\}, \quad y \in \{1, \ldots, N\}. \tag{10}$$

The SNR is the ratio of the signal power to the power of the noise corrupting the signal and can be written as (11) in which P_S is the optical signal power and P_N is the power of noise

$$SNR = 10 \log \left(\frac{P_S}{P_N} \right). \tag{11}$$

III. Network Level Analysis

We analyze the worst-case crosstalk noise and SNR of the mesh-based ONoCs using the proposed general optical router model. When an optical signal passes through an optical router, it suffers from power loss. The maximum loss link has the longest length and includes the maximum number of optical routers. By contrast, the minimum loss link includes the minimum number of optical routers and has the shortest length. The minimum SNR link determines the feasibility of an ONoC. Two major conditions should be taken into consideration for analyzing the minimum SNR link. First, the minimum SNR link should suffer from high power loss. Second, it should suffer from high crosstalk noise introduced by other optical links. Therefore, the longest optical link with

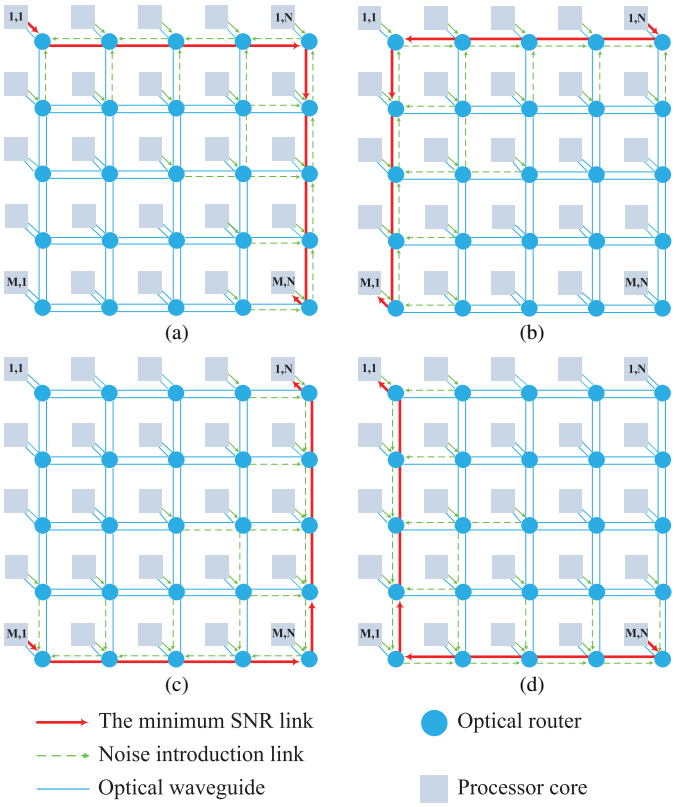

Fig. 4. First longest optical link in an $M \times N$ 2-D mesh-based ONoC. (a) (1, 1) to (M, N). (b) (1, N) to (M, 1). (c) (M, 1) to (1, N). (d) (M, N) to (1, 1).

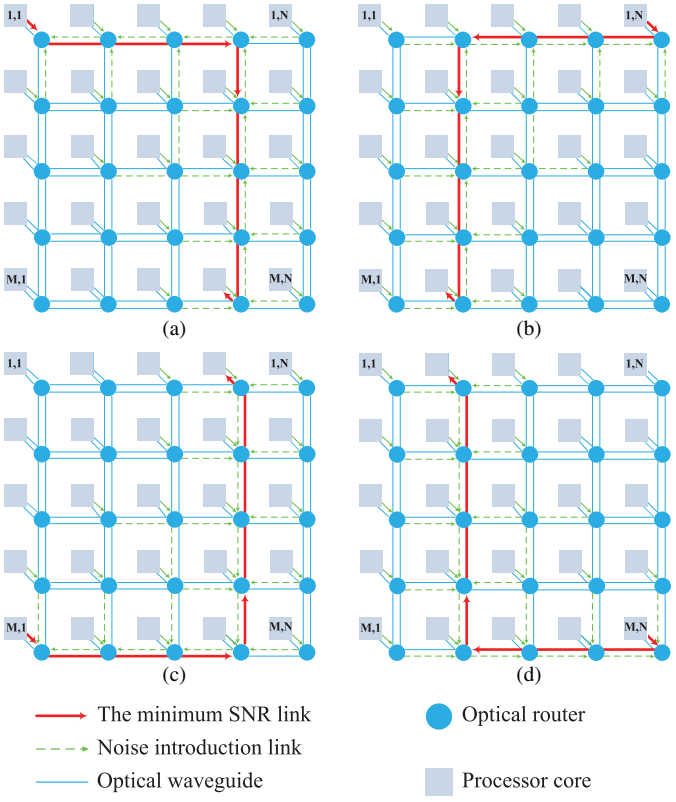

Fig. 5. Second longest optical link in an $M \times N$ 2-D mesh-based ONoC. (a) (1, 1) to (M, N-1). (b) (1, N) to (M, 2). (c) (M, 1) to (1, N-1). (d) (M, N) to (1, 2).

the maximum power loss may not be the minimum SNR link since shorter optical links may suffer from higher crosstalk noise which results in worse SNR. Based on these conditions, we analyze different longest optical links in the mesh-based ONoCs to find the minimum SNR link. Dimension-order routing is used in the network.

A. SNR Analyses of Different Longest Optical Links

We consider some assumptions to make the worst-case crosstalk noise analysis possible. In the mesh-based ONoCs, it can be presumed that the optical signal loss for the same input and output pair but in different routers is the same as shown in (12). Therefore, $L_{i,j}(x, y)$ can be simplified as $L_{i,j}$ which is the loss for the optical signal traveling from the ith input port toward the jth output port independent of the optical router location. Multiplying $K_{i,j,m}$ by another crosstalk coefficient results in a very small number which can be estimated as zero (13). We also assume that the optical signal power at the injection ports of different optical routers is the same. Another assumption used in this paper is explained in (14). These assumptions are used in all of the analyses in this paper

$$L_{i,j}(x_0, y_0) = L_{i,j}(x_1, y_1) = L_{i,j} \tag{12}$$

$$K_{i_0,j_0,m_0} K_{i_1,j_1,m_1} \approx 0, \quad i_0, j_0, m_0, i_1, j_1, m_1 \in \{0, \ldots, 4\} \tag{13}$$

$$L_{0,j_0} \geq L_{0,j_1} L_{(j_1+1) mod 4+1, j_0}, \quad j_0, j_1 \in \{1, \ldots, 4\}. \tag{14}$$

We start with the first longest optical link in the network. The power loss of the optical signal traveling from the processor core (x_0, y_0) to the core (x_1, y_1) is defined in (15) in which P is the input optical power and L is the optical signal loss. Fig. 4 illustrates the first longest optical links in the mesh-based ONoCs. The power loss of the first optical link, shown in Fig. 4(a), is calculated in (16). In this equation, P_{in} is the input optical power

$$PL_{(x_0,y_0),(x_1,y_1)} \quad x_0, x_1 \in \{1, \ldots, M\}, y_0, y_1 \in \{1, \ldots, N\} \tag{15}$$

$$PL_{(1,1),(M,N)} = P_{\text{in}} L_{0,2} L_{4,2}^{N-2} L_{4,3} L_{1,3}^{M-2} L_{1,0}. \tag{16}$$

In Fig. 4, the dashed green lines show the optical links which introduce crosstalk noise to the minimum SNR link. The communication pattern among the processor cores, shown in the dashed green lines, is considered in the way to make the received crosstalk noise at the destination of different longest optical links as high as possible (the worst-case). In Fig. 4(a), as an example, for the optical router $R(1, 1)$, the optical signal traveling from the injection port to the east port can be corrupted by the optical signals from the neighboring routers into the south and east ports. Considering the location of the router, it is obvious that $K_{0,2,1}$ and $K_{0,2,4}$, which are the crosstalk coefficients introduced by P_1^0 (into the north port) and P_4^0 (into the west port), are zero. Based on (10), we can define $N_{0,2}(1, 1) = P_2^0 K_{0,2,2} + P_3^0 K_{0,2,3}$ as the crosstalk noise added to the optical signal traveling from the injection to the east port in the router $R(1, 1)$. The optical signal that introduces crosstalk noise to the router $R(1, 1)$, travels from the injection port to the west

$$N_{i,j\,(1st)}(x,y,ws_{i,j}(x,y)) = \begin{cases} P_{\text{in}}(L_{0,4}K_{0,2,2}+L_{0,1}K_{0,2,3}), & x=1,y=1,i=0,j=2 \\ P_{\text{in}}(K_{4,2,0}+L_{0,4}K_{4,2,2}+L_{0,1}K_{4,2,3}), & x=1,y\in(1,N-1),i=4,j=2 \\ P_{\text{in}}(K_{4,2,0}+L_{0,4}K_{4,2,2}+L_{0,2}L_{4,1}L_{3,1}K_{4,2,3}), & x=1,y=N-1,i=4,j=2 \\ P_{\text{in}}(K_{4,3,0}+L_{0,1}K_{4,3,3}), & x=1,y=N,i=4,j=3 \\ P_{\text{in}}(K_{1,3,0}+L_{0,1}K_{1,3,3}+L_{0,2}K_{1,3,4}), & x\in(1,M),y=N,i=1,j=3 \\ P_{\text{in}}(K_{1,0,0}+L_{0,2}K_{1,0,4}), & x=M,y=N,i=1,j=0 \end{cases} \tag{17}$$

$$N_{i,j\,(2nd)}(x,y,ws_{i,j}(x,y)) = \begin{cases} P_{\text{in}}(L_{0,4}K_{0,2,2}+L_{0,1}K_{0,2,3}), & x=1,y=1,i=0,j=2 \\ P_{\text{in}}(K_{4,2,0}+L_{0,4}K_{4,2,2}+L_{0,1}K_{4,2,3}), & x=1,y\in(1,N-2),i=4,j=2 \\ P_{\text{in}}(K_{4,2,0}+L_{0,4}K_{4,2,2}+L_{0,2}L_{4,1}L_{3,1}K_{4,2,3}), & x=1,y=N-2,i=4,j=2 \\ P_{\text{in}}(K_{4,3,0}+L_{0,4}K_{4,3,2}+L_{0,1}K_{4,3,3}), & x=1,y=N,i=4,j=3 \\ P_{\text{in}}(K_{1,3,0}+L_{0,1}K_{1,3,3}+L_{0,2}K_{1,3,4}+L_{0,4}K_{1,3,2}), & x\in(1,M),y=N,i=1,j=3 \\ P_{\text{in}}(K_{1,0,0}+L_{0,2}K_{1,0,4}+L_{0,4}K_{1,0,2}), & x=M,y=N,i=1,j=0 \end{cases} \tag{20}$$

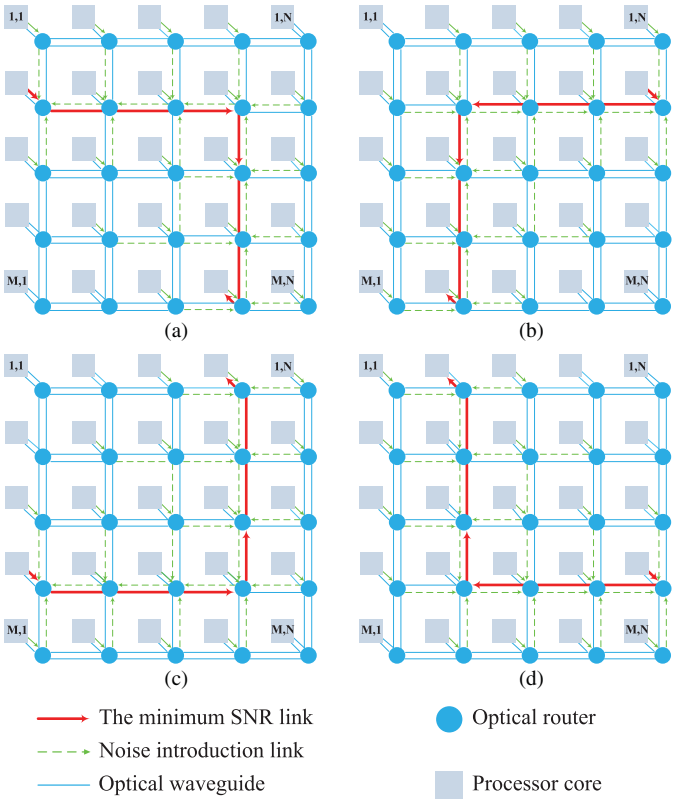

Fig. 6. Third longest optical link in an $M \times N$ 2-D mesh-based ONoC. (a) (2, 1) to (M, N-1). (b) (2, N) to (M, 2). (c) (M-1, 1) to (1, N-1). (d) (M-1, N) to (1, 2).

port in the optical router $R(1, 2)$, then reaches the east port in the optical router $R(1, 1)$ and then mixes with the optical signal traveling from the injection port to the east port. The power of the optical signal injected into the east port of the optical router $R(1, 1)$ can be calculated as $P_2^0 = P_{\text{in}}L_{0,4}$. Following the same principle, the power of optical signal injected into the south port can be written as $P_3^0 = P_{\text{in}}L_{0,1}$. The crosstalk noise for the other optical routers can be calculated following the same procedure.

Using (10), Fig. 4(a), and the aforementioned analyses, the crosstalk noise introduced at the optical routers $R(1, y)$ on the X-section and at the optical routers $R(x, N)$ on the Y-section of the first longest link is calculated in (17), as shown at the top of the page. $ws_{i,j}(x,y)$ is also considered as the worst-case status of the router $R(x, y)$ while considering statuses of other routers to guaranty the worst-case crosstalk noise analysis condition.

Considering (11), (16), and (17), the SNR of the longest optical link traveling from the processor core (1, 1) toward the core (M, N) in the mesh-based ONoCs can be written as (18). The same procedure can be applied to analyze the SNR of the other three first longest optical links indicated in Fig. 4

$$SNR_{(1,1),(M,N)} = 10\log\left(\frac{PL_{(1,1),(M,N)}}{P_{N1}}\right) \tag{18}$$

$$\begin{aligned} P_{N1} &= N_{0,2}(1,1)L_{4,2}^{N-2}L_{4,3}L_{1,3}^{M-2}L_{1,0} \\ &+L_{4,3}L_{1,3}^{M-2}L_{1,0}L_{4,2}\left(\sum_{j=2}^{N-2}L_{4,2}^{N-2-j}N_{4,2}(1,2)\right) \\ &+N_{4,2}(1,N-1)L_{4,3}L_{1,3}^{M-2}L_{1,0}+N_{4,3}(1,N)L_{1,3}^{M-2}L_{1,0} \\ &+L_{1,0}\left(\sum_{i=2}^{M-1}L_{1,3}^{M-1-i}N_{1,3}(2,N)\right)+N_{1,0}(M,N) \end{aligned}$$

$$PL_{(1,1),(M,N-1)} = P_{\text{in}}L_{0,2}L_{4,2}^{N-3}L_{4,3}L_{1,3}^{M-2}L_{1,0} \tag{19}$$

$$SNR_{(1,1),(M,N-1)} = 10\log\left(\frac{PL_{(1,1),(M,N-1)}}{P_{N2}}\right) \tag{21}$$

$$\begin{aligned} P_{N2} &= N_{0,2}(1,1)L_{4,2}^{N-3}L_{4,3}L_{1,3}^{M-2}L_{1,0} \\ &+L_{4,3}L_{1,3}^{M-2}L_{1,0}L_{4,2}\left(\sum_{j=2}^{N-3}L_{4,2}^{N-3-j}N_{4,2}(1,2)\right) \\ &+N_{4,2}(1,N-2)L_{4,3}L_{1,3}^{M-2}L_{1,0}+N_{4,3}(1,N-1)L_{1,3}^{M-2}L_{1,0} \\ &+L_{1,0}\left(\sum_{i=2}^{M-1}L_{1,3}^{M-1-i}N_{1,3}(2,N-1)\right)+N_{1,0}(M,N-1). \end{aligned}$$

The second longest optical link needs to be considered as well. There are totally 16 optical links with the second longest length in the mesh-based ONoCs. Among these links, four of them, which are shown in Fig. 5, have the worst-case crosstalk noise. The power loss of the second longest optical link, shown in Fig. 5(a), is calculated in (19)

$$PL_{(2,1),(M,N-1)} = P_{\text{in}}L_{0,2}L_{4,2}^{N-3}L_{4,3}L_{1,3}^{M-3}L_{1,0}. \tag{22}$$

$$N_{i,j\,(3rd)}(x,y,ws_{i,j}(x,y))=\begin{cases}P_{\text{in}}(L_{0,3}K_{0,2,1}+L_{0,4}K_{0,2,2}+L_{0,1}K_{0,2,3}), & x=2,\ y=1,\ i=0,\ j=2\\ P_{\text{in}}(K_{4,2,0}+L_{0,3}K_{4,2,1}+L_{0,4}K_{4,2,2}+L_{0,1}K_{4,2,3}), & x=2,\ y\in(1,N-2),\ i=4,\ j=2\\ P_{\text{in}}(K_{4,2,0}+L_{0,3}K_{4,2,1}+L_{0,4}K_{4,2,2}+L_{0,2}L_{4,1}L_{3,1}K_{4,2,3}), & x=2,\ y=N-2,\ i=4,\ j=2\\ P_{\text{in}}(K_{4,3,0}+L_{0,3}K_{4,3,1}+L_{0,4}K_{4,3,2}+L_{0,1}K_{4,3,3}), & x=2,\ y=N-1,\ i=4,\ j=3\\ P_{\text{in}}(K_{1,3,0}+L_{0,4}K_{1,3,2}+L_{0,1}K_{1,3,3}+L_{0,2}K_{1,3,4}), & x\in(2,M),\ y=N-1,\ i=1,\ j=3\\ P_{\text{in}}(K_{1,0,0}+L_{0,2}K_{1,0,4}+L_{0,4}K_{1,0,2}), & x=M,\ y=N-1,\ i=1,\ j=0\end{cases} \tag{23}$$

$$N_{i,j\,(4th)}(x,y,ws_{i,j}(x,y))=\begin{cases}P_{\text{in}}(L_{0,3}K_{0,2,1}+L_{0,4}K_{0,2,2}+L_{0,1}K_{0,2,3}), & x=2,\ y=1,\ i=0,\ j=2\\ P_{\text{in}}(K_{4,2,0}+L_{0,3}K_{4,2,1}+L_{0,4}K_{4,2,2}+L_{0,1}K_{4,2,3}), & x=2,\ y\in(1,N-3),\ i=4,\ j=2\\ P_{\text{in}}(K_{4,2,0}+L_{0,3}K_{4,2,1}+L_{0,4}K_{4,2,2}+L_{0,2}L_{4,1}L_{3,1}K_{4,2,3}), & x=2,\ y=N-3,\ i=4,\ j=2\\ P_{\text{in}}(K_{4,3,0}+L_{0,3}K_{4,3,1}+L_{0,4}K_{4,3,2}+L_{0,1}K_{4,3,3}), & x=2,\ y=N-2,\ i=4,\ j=3\\ P_{\text{in}}(K_{1,3,0}+L_{0,4}K_{1,3,2}+L_{0,1}K_{1,3,3}+L_{0,2}K_{1,3,4}), & x\in(2,M),\ y=N-2,\ i=1,\ j=3\\ P_{\text{in}}(K_{1,0,0}+L_{0,2}K_{1,0,4}+L_{0,4}K_{1,0,2}), & x=M,\ y=N-2,\ i=1,\ j=0\end{cases} \tag{26}$$

Based on (10), Fig. 5(a), and by following the same principles discussed for the first longest optical link, the crosstalk noise introduced at the optical routers $R(1, y)$ on the X-section and at the optical routers $R(x, N-1)$ on the Y-section of the second longest optical link is calculated in (20). Using (11), (19), and (20), the SNR of the second longest optical link traveling from the processor core (1, 1) toward the core $(M, N-1)$ in the mesh-based ONoCs is calculated in (20).

Fig. 6 shows four links out of 36 different third longest optical links, which have the worst-case crosstalk noise in the network. The power loss of the first optical link, shown in Fig. 6(a), is defined in (22). Considering (10) and Fig. 6(a), the crosstalk noise introduced at the optical routers $R(2, y)$ on the X-section and at the optical routers $R(x, N-1)$ on the Y-section of the third longest optical link is calculated in (23), as shown at the top of the page. According to (11), (22), and (23), the SNR of the third longest optical link traveling from the processor core (2, 1) toward the core $(M, N-1)$ in the mesh-based ONoCs can be written as (24)

$$SNR_{(2,1),(M,N-1)}=10\log\left(\frac{PL_{(2,1),(M,N-1)}}{P_{N3}}\right) \tag{24}$$

$$\begin{aligned}P_{N3}&=N_{0,2}(2,1)L_{4,2}^{N-3}L_{4,3}L_{1,3}^{M-3}L_{1,0}\\&+L_{4,3}L_{1,3}^{M-3}L_{1,0}L_{4,2}\left(\sum_{j=2}^{N-3}L_{4,2}^{N-3-j}N_{4,2}(2,2)\right)\\&+N_{4,2}(1,N-2)L_{4,3}L_{1,3}^{M-3}L_{1,0}\\&+N_{4,3}(2,N-1)L_{1,3}^{M-3}L_{1,0}\\&+L_{1,0}\left(\sum_{i=3}^{M-1}L_{1,3}^{M-1-i}N_{1,3}(3,N-1)\right)+N_{1,0}(M,N-1)\end{aligned}$$

$$PL_{(2,1),(M,N-2)}=P_{\text{in}}L_{0,2}L_{4,2}^{N-4}L_{4,3}L_{1,3}^{M-3}L_{1,0} \tag{25}$$

$$SNR_{(2,1),(M,N-2)}=10\log\left(\frac{PL_{(2,1),(M,N-2)}}{P_{N4}}\right) \tag{27}$$

$$\begin{aligned}P_{N4}&=N_{0,2}(2,1)L_{4,2}^{N-4}L_{4,3}L_{1,3}^{M-3}L_{1,0}\\&+L_{4,3}L_{1,3}^{M-3}L_{1,0}L_{4,2}\left(\sum_{j=2}^{N-4}L_{4,2}^{N-4-j}N_{4,2}(2,2)\right)\\&+N_{4,2}(2,N-2)L_{4,3}L_{1,3}^{M-3}L_{1,0}\\&+N_{4,3}(2,N-2)L_{1,3}^{M-3}L_{1,0}\\&+L_{1,0}\left(\sum_{i=3}^{M-1}L_{1,3}^{M-1-i}N_{1,3}(3,N-2)\right)+N_{1,0}(M,N-2).\end{aligned}$$

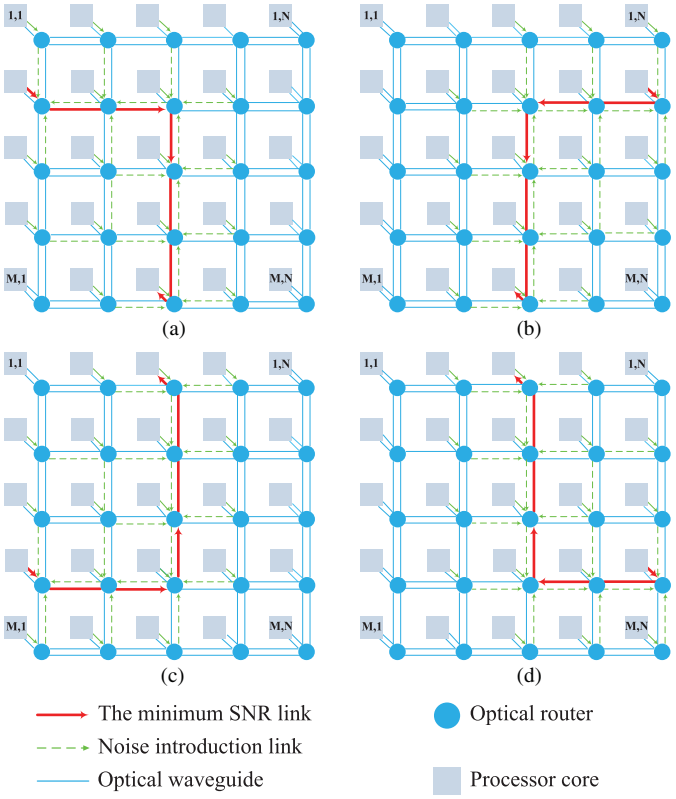

Fig. 7. Fourth longest optical link in an $M \times N$ 2-D mesh-based ONoC. (a) (2, 1) to (M, N-2). (b) (2, N) to (M, 3). (c) (M-1, 1) to (1, N-2). (d) (M-1, N) to (1, 3).

The fourth longest optical links, shown in Fig. 7, are selected since they have the worst-case crosstalk noise compared with the other possible fourth longest links. The power loss of the first optical link, shown in Fig. 7(a), is calculated in (24) According to (10) and Fig. 6(a), the crosstalk noise introduced at the optical routers $R(2, y)$ on the X-section and at the optical routers $R(x, N-2)$ on the Y-section of the fourth longest optical link is shown in (26), as shown at the top of the page. Using (11), (24), and (26), the SNR of the fourth longest optical link traveling from the processor core (2, 1) toward the core $(M, N-2)$ in the mesh-based ONoCs is defined (27).

Finally, we need to consider the fifth longest optical link in the mesh-based ONoCs. Four of the fifth longest optical links which have the worst-case crosstalk noise compared with other possible fifth longest links are shown in Fig. 8. The power loss

$$N_{i,j\,(5th)}(x,y,ws_{i,j}(x,y)) = \begin{cases} P_{\text{in}}(L_{0,3}K_{0,2,1} + L_{0,4}K_{0,2,2} + L_{0,1}K_{0,2,3}), & x=3, y=1, i=0, j=2 \\ P_{\text{in}}(K_{4,2,0} + L_{0,3}K_{4,2,1} + L_{0,4}K_{4,2,2} + L_{0,1}K_{4,2,3}), & x=3, y\in(1,N-3), i=4, j=2 \\ P_{\text{in}}(K_{4,2,0} + L_{0,3}K_{4,2,1} + L_{0,4}K_{4,2,2} + L_{0,2}L_{4,1}L_{3,1}K_{4,2,3}), & x=3, y=N-3, i=4, j=2 \\ P_{\text{in}}(K_{4,3,0} + L_{0,3}K_{4,3,1} + L_{0,4}K_{4,3,2} + L_{0,1}K_{4,3,3}), & x=3, y=N-2, i=4, j=3 \\ P_{\text{in}}(K_{1,3,0} + L_{0,4}K_{1,3,2} + L_{0,1}K_{1,3,3} + L_{0,2}K_{1,3,4}), & x\in(3,M), y=N-2, i=1, j=3 \\ P_{\text{in}}(K_{1,0,0} + L_{0,2}K_{1,0,4} + L_{0,4}K_{1,0,2}), & x=M, y=N-2, i=1, j=0 \end{cases} \quad (29)$$

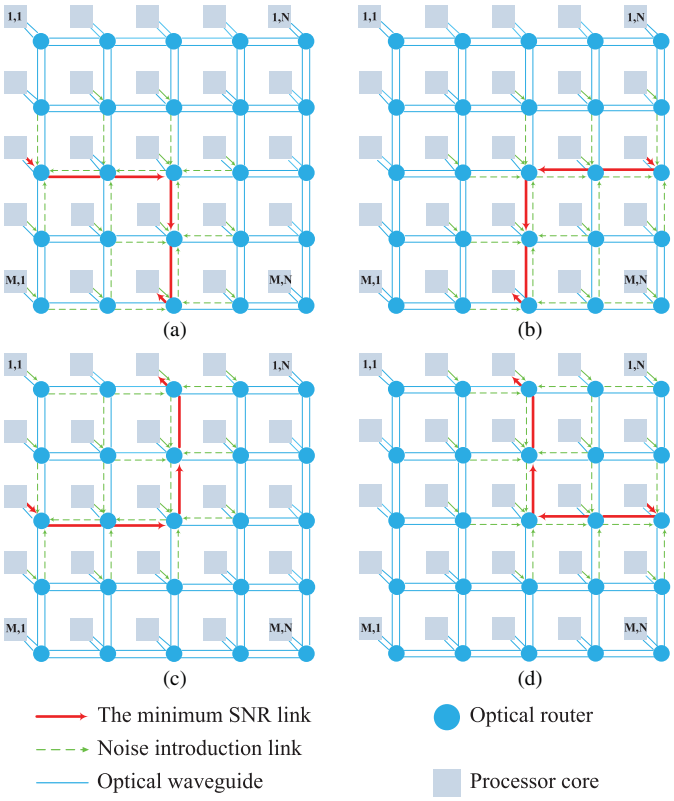

Fig. 8. Fifth longest optical link in an $M \times N$ 2-D mesh-based ONoC. (a) (3, 1) to (M, N-2). (b) (3, N) to (M, 3). (c) (M-2, 1) to (1, N-2). (d) (M-2, N) to (1, 3).

of the first optical link, shown in Fig. 8(a), is calculated in (28)

$$PL_{(3,1),(M,N-2)} = P_{\text{in}}L_{0,2}L_{4,2}^{N-4}L_{4,3}L_{1,3}^{M-4}L_{1,0} \quad (28)$$

$$SNR_{(3,1),(M,N-2)} = 10\log\left(\frac{PL_{(3,1),(M,N-2)}}{P_{N5}}\right) \quad (30)$$

$$\begin{aligned} P_{N5} = {} & N_{0,2}(3,1)L_{4,2}^{N-4}L_{4,3}L_{1,3}^{M-4}L_{1,0} \\ & + L_{4,3}L_{1,3}^{M-4}L_{1,0}L_{4,2}\left(\sum_{j=2}^{N-4}L_{4,2}^{N-4-j}N_{4,2}(3,2)\right) \\ & + N_{4,2}(2,N-3)L_{4,3}L_{1,3}^{M-4}L_{1,0} \\ & + N_{4,3}(3,N-2)L_{1,3}^{M-4}L_{1,0} \\ & + L_{1,0}\left(\sum_{i=4}^{M-1}L_{1,3}^{M-1-i}N_{1,3}(4,N-2)\right) \\ & + N_{1,0}(M,N-2). \end{aligned}$$

Based on (10) and Fig. 8(a), the crosstalk noise introduced at the optical routers $R(3, y)$ on the X-section and at the optical routers $R(x, N-2)$ on the Y-section of the fifth longest link is defined in (29), as shown at the top of the page. Considering (11), (28), and (29), the SNR of the fifth longest optical link traveling from the processor core (3, 1) to the core $(M, N-2)$ in the mesh-based ONoCs is defined in (28).

B. Minimum SNR Link in the Mesh-Based ONoCs

In this section, an effort is made to find the minimum SNR link candidates among the analyzed optical links. According to Fig. 4, the whole path (X-section and Y-section) of the first longest optical link is located at the network edge. In general, this fact results in less crosstalk noise based on the second condition for the minimum SNR link in the mesh-based ONoCs. The same fact applies to the X-section of the second longest optical link. Although the Y-section can satisfy the second condition, the X-section is at the network edge and suffers from less crosstalk noise. We call the optical links located at the network edge as edge links. On the other hand, considering Figs. 6–8, the whole optical link path lies inside the network. We call these links as internal links. The crosstalk noise added to the internal links follows the same pattern in the mesh-based ONoCs. Therefore, the SNR of the internal links relies on the length of the optical link. That is, it can be proved that by moving further from the first internal link (third longest optical link) toward inside the network, optical links become shorter which results in less optical loss and consequently better SNR.

We try to find the minimum SNR link between the fourth and the fifth longest optical links, whose SNRs are defined in (27) and (30). By grouping the numerator and denominator in (27) into different parameters, we obtain

$$SNR_{(2,1),(M,N-2)} = 10\log\left(\frac{a}{b_1+b_2+b_3+b_4}\right) \quad (31)$$

where

$$\begin{aligned} a = {} & L_{0,2}L_{4,2}^{N-4}L_{4,3}L_{1,3}^{M-3}L_{1,0} \\ b_1 = {} & L_{4,2}^{N-4}L_{4,3}L_{1,3}^{M-3}L_{1,0}(L_{0,3}K_{0,2,1} + L_{0,4}K_{0,2,2} \\ & + L_{0,1}K_{0,2,3}) \\ b_2 = {} & L_{4,3}L_{1,3}^{M-3}L_{1,0}L_{4,2}\left(\frac{1-L_{4,2}^{N-5}}{1-L_{4,2}}\right)(K_{4,2,0} + L_{0,3}K_{4,2,1} \\ & + L_{0,4}K_{4,2,2} + L_{0,1}K_{4,2,3}) + L_{4,3}L_{1,3}^{M-3}L_{1,0}(K_{4,2,0} \\ & + L_{0,3}K_{4,2,1} + L_{0,4}K_{4,2,2} + L_{0,2}L_{4,1}L_{3,1}K_{4,2,3}) \\ & + L_{1,3}^{M-3}L_{1,0}(K_{4,3,0} + L_{0,3}K_{4,3,1} + L_{0,4}K_{4,3,2} \\ & + L_{0,1}K_{4,3,3}) \\ b_3 = {} & L_{1,0}\left(\frac{1-L_{1,3}^{M-3}}{1-L_{1,3}}\right)(K_{1,3,0} + L_{0,4}K_{1,3,2} + L_{0,1}K_{1,3,3} \\ & + L_{0,2}K_{1,3,4}) \\ b_4 = {} & (K_{1,0,0} + L_{0,2}K_{1,0,4} + L_{0,4}K_{1,0,2}). \end{aligned}$$

Considering (31), the SNR of the fifth longest optical link, shown in (30), can be represented as

$$SNR^{-1}_{(3,1),(M,N-2)} = 0.1\log^{-1}\left(\frac{L_{1,3}^{-1}b_1+L_{1,3}^{-1}b_2+b_3}{L_{1,3}^{-1}a}+\frac{b_4-N_{1,3}(3,N-2)L_{1,0}L_{1,3}^{M-4}}{L_{1,3}^{-1}a}\right) = 0.1\log^{-1}\left(\frac{k(b_1+b_2)+b_3+b_4-C}{ka}\right) \quad (32)$$

where

$$k = L_{1,3}^{-1}$$
$$C = N_{1,3}(3,N-2)L_{1,0}L_{1,3}^{M-4}.$$

According to (32), because a, b_1, b_2, b_3, b_4, and C are positive numbers and $k \geq 1$, we can easily conclude (33). In this equation, the left side indicates the SNR of the fourth longest link while the right side is the SNR of the fifth longest link. Based on (33), the SNR of the fourth longest optical link is smaller than the SNR of the fifth longest optical link in the mesh-based ONoCs. Following the same principle as shown in (33), it can be seen that the SNR of the third longest optical link is smaller than the forth longest optical link in the mesh-based ONoCs. In this equation, the left side indicates the simplified SNR of the third longest optical link and the right side is the SNR of the fourth longest optical link. C' equals to $L_{4,3}L_{1,3}^{M-3}L_{1,0}L_{4,2}^{N-4}$, and k' equals to $L_{4,2}$. It can be seen that $C' \geq 0$ and $k' \leq 1$

$$\frac{a}{b_1+b_2+b_3+b_4} \leq \frac{ka}{k(b_1+b_2)+b_3+b_4-C} \quad (33)$$

$$\frac{k'a}{k'b_1+b_2+b_3+b_4+C'} \leq \frac{a}{b_1+b_2+b_3+b_4}. \quad (34)$$

Regarding Figs. 6 and 7, both of the third and the fourth longest optical links are internal links. The crosstalk noise introduced to these links follows the same pattern (second condition). Therefore, since the third longest optical link is longer than the fourth one, which results in higher power loss, the SNR of the third longest optical link is smaller than the fourth longest link which is mathematically proved as well. The same conclusion can be applied to other longest optical links shorter than the fifth longest link

$$SNR^{-1}_{(1,1),(M,N)} = 0.1\log^{-1}\left(\frac{K(1+L+L^2-L^M)}{(1-L)L^{N+M-1}}+\frac{K(L^{M+2}+L^{M+3}-L^{M+4})}{(1-L)L^{N+M-1}}-\frac{K(L^{N+M-2}+2L^{N+M})}{(1-L)L^{N+M-1}}\right) \quad (35)$$

$$SNR^{-1}_{(1,1),(M,N-1)} = 0.1\log^{-1}\left(\frac{K(1+2L+L^2-L^M)}{(1-L)L^{N+M-2}}+\frac{K(L^{M+2}-L^{M+1}+L^{M+3})}{(1-L)L^{N+M-2}}-\frac{K(L^{M+4}-L^{N+M-2})}{(1-L)L^{N+M-2}}-\frac{K(4L^{N+M-1})}{(1-L)L^{N+M-2}}\right) \quad (36)$$

TABLE II
LOSS VALUES, CROSSTALK, AND REFLECTANCE COEFFICIENTS

Parameter	Value	Reference
L_c	–0.04 dB	[12]
L_p	–0.274 dB/cm	[17]
$L_{c,\text{off}}$	–0.04 dB	-
$L_{c,\text{on}}$	–0.5 dB	-
L_b	–0.005 dB/90°	[5]
$L_{p,\text{off}}$	–0.005 dB	[13]
$L_{p,\text{on}}$	–0.5 dB	[13]
K_c	–40 dB	[12]
$K_{p,\text{off}}$	–20 dB	[13]
$K_{p,\text{on}}$	–25 dB	[13]
K_r	$\cong 0$	[12]
K_t	–50 dB	[18]

$$SNR^{-1}_{(2,1),(M,N-1)} = 0.1\log^{-1}\left(\frac{K(1+2L+L^2-L^M)}{(1-L)L^{N+M-3}}+\frac{K(L^{M+1}+L^{M+2}-L^{M+3})}{(1-L)L^{N+M-3}}-\frac{K(L^{M+N-4}+3L^{M+N-2})}{(1-L)L^{N+M-3}}\right). \quad (37)$$

According to the mentioned analyses, it is proved that the minimum SNR link in the mesh-based ONoCs should be among the first, the second, and the third longest optical links. From each group of four worst-case longest optical links, we picked the first link as a candidate for our analyses. The analyses for the other three optical links in each group are the same and result in the same conclusion drawn here.

IV. NUMERICAL SIMULATION

In this section, we present the numerical simulations of the minimum SNR link candidates performed using MATLAB. Table II shows the example values for the power loss values, crosstalk coefficients, and reflection coefficients used in this section and also later in our case study. As mentioned before, $L_{c,\text{off}}$ and $L_{c,\text{on}}$ can be calculated based on the other parameters. It needs to be noted that in order to perfectly indicate the results, all of the vertical axes are reversed in this section as well as in the next one.

The insertion losses as well as the crosstalk noise coefficients are supposed to be equal to simplify SNR equations. That is, $L_{i,j} = L$ and $K_{i,j,m} = K$ while K is the arithmetic mean of different crosstalk noise coefficients K_c, $K_{p,\text{off}}$, and $K_{p,\text{on}}$ shown in Table II. Therefore, (18), (20), and (24) can be simplified as (35)–(37), respectively. In these equations, L corresponds to the insertion loss and K shows the crosstalk coefficient.

Fig. 9(a)–(c) shows the SNR of the first, the second, and the third longest optical links based on the simplified equations and under the three loss values of -0.1, -0.2, and -0.3 dB. The increase in the network size results in the increase in the number of optical routers included in the optical link and, consequently, smaller SNR. Moreover, the higher the loss value, the smaller the SNR is. Furthermore, it can be seen that

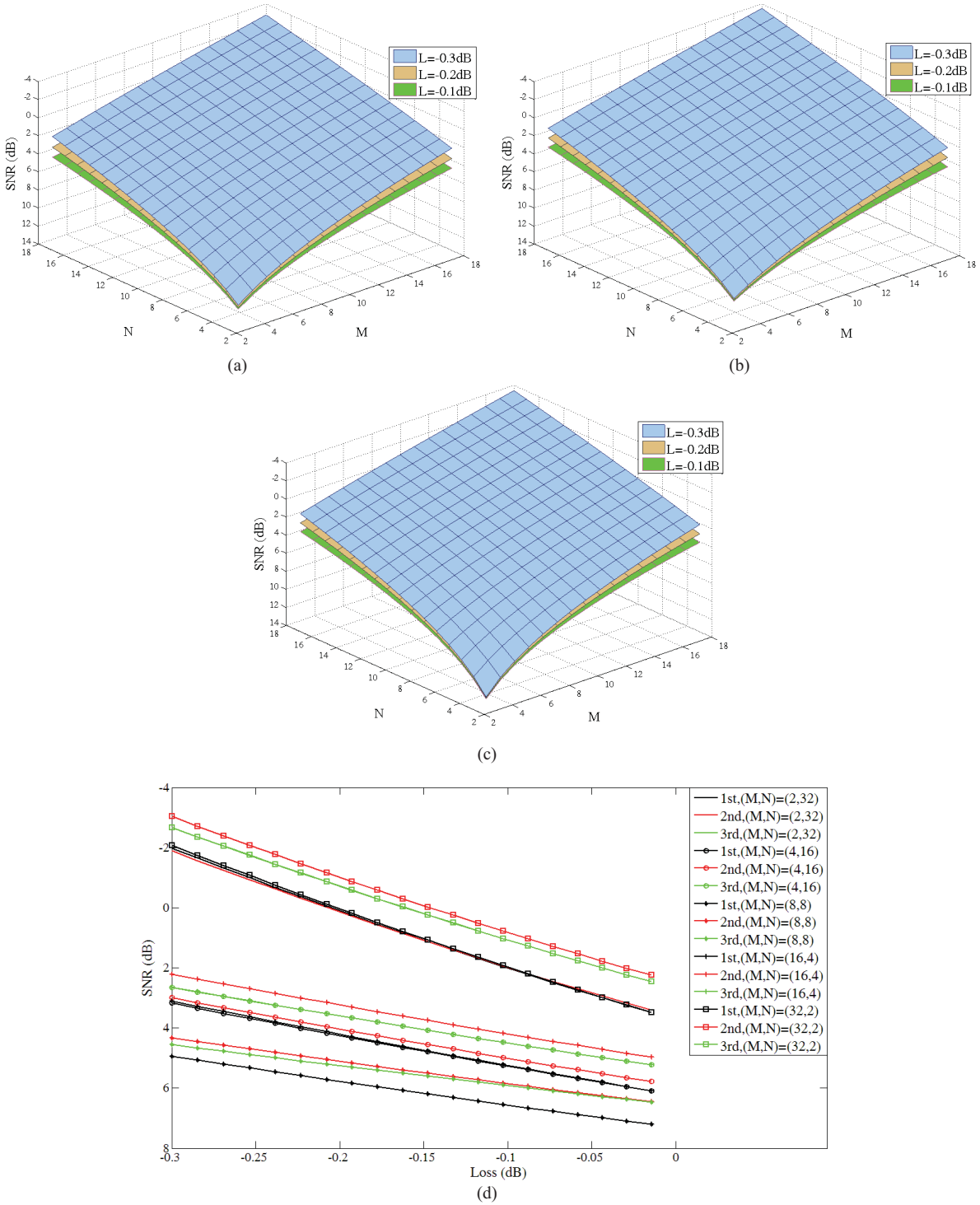

Fig. 9. SNR comparison among the first, the second, and the third longest optical links in an $M \times N$ mesh-based ONoC. (a) First longest optical link. (b) Second longest optical link. (c) Third longest optical link. (d) $M \times N = 64$.

the SNR is the best when $M = N$. Suppose $M \times N = C$ and C is constant; according to the SNR equations, the best SNR can be achieved only when $M = N$. That is, a symmetric mesh-based network has the best SNR performance. Fig. 9(d) compares the SNR of the first, the second, and the third longest optical links when $C = 64$ and it shows that the best SNR can be achieved only when $M = N = 8$. Moreover, the closer M and N results in better SNR.

The relationship between the SNR and the loss among the first, the second, and the third longest optical links for the loss ranges from -1.5 to 0 dB for three different network sizes is shown in Fig. 10. There are four different regions specified by the crossing points in this figure. Table III summarizes the SNR comparison among the first, the second, and the third longest optical links in different regions shown in Fig. 10. As the table shows, the minimum SNR link can be the first or

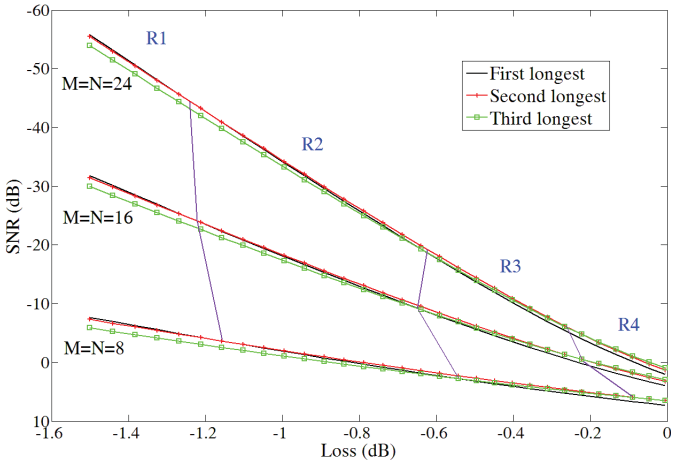

Fig. 10. Relationship between SNR and the loss among the first, the second, and the third longest optical links in an $M \times N$ mesh-based ONoC.

TABLE III
SNR COMPARISON IN FIG. 10

Region	SNR Comparison
R1	$SNR_{1st} < SNR_{2nd} < SNR_{3rd}$
R2	$SNR_{2nd} < SNR_{1st} < SNR_{3rd}$
R3	$SNR_{2nd} < SNR_{3rd} < SNR_{1st}$
R4	$SNR_{3rd} < SNR_{2nd} < SNR_{1st}$

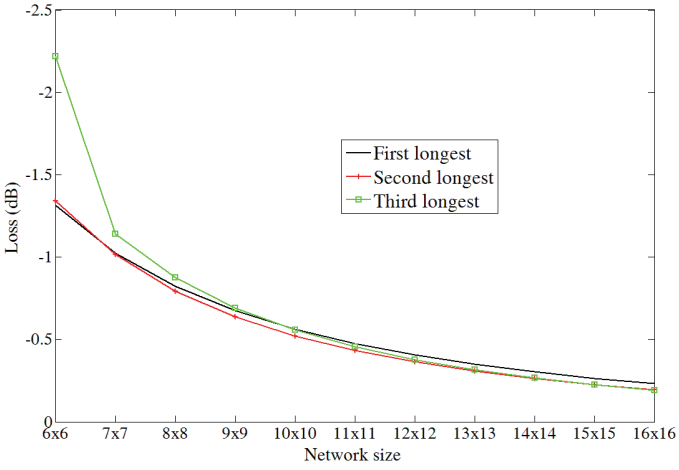

Fig. 11. Relationship between loss and network size when signal power is equal to noise power (SNR = 0 dB).

the second or the third longest optical link depends on the value of L. For example, when -1.5 dB $\leq L < -1.2$ dB, the first longest optical link is the minimum SNR link in the network (the first region); but when -0.2 dB $\leq L < 0$ dB, the third longest optical link is the minimum SNR link (the fourth region).

Fig. 11 shows the relationship between the power loss and the network size when the signal power equals to the noise power (SNR = 0 dB). As can be seen from the figure, the power loss decreases quickly when the network size increases. Given a network size and its related loss value in the figure, the noise power exceeds the signal power for higher loss values.

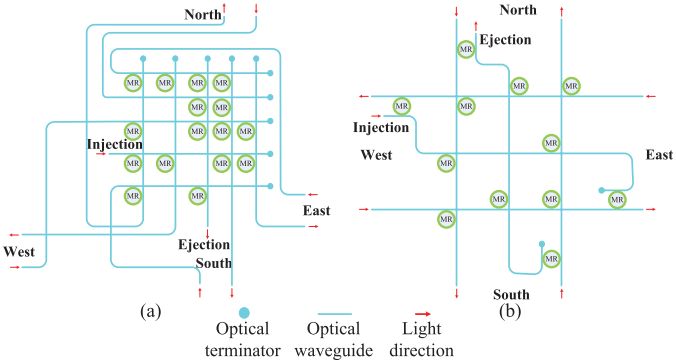

Fig. 12. (a) Optimized optical crossbar router. (b) Crux optical router.

Furthermore, in mesh-based ONoCs with the network sizes larger than 16×16, the crosstalk noise power is higher than the signal power, which indicates the critical behavior of crosstalk noise in large scale ONoCs.

V. CASE STUDY

The SNR of the $M \times N$ mesh-based ONoCs using optimized crossbar and Crux optical routers is analyzed based on the proposed formal method. We developed an automated crosstalk analyzer, called CLAP, for optical routers based on the analyses of the basic optical devices and optical switching elements.

Fig. 12 shows the optimized crossbar and Crux optical routers structures. Both routers have five bidirectional ports, including- Injection/Ejection, East, South, West, and North. The Injection/Ejection port is connected to a local processor core through an optical/electronic (O/E) interface. The analyses indicate that the first longest optical link from the processor core $(1, N)$ to the core $(M, 1)$ is the minimum SNR link in the mesh-based ONoCs using optimized optical crossbar router. However, when Crux optical router is used, the minimum SNR link is the second longest optical link from the processor core $(1, N)$ toward the core $(M, 2)$ in the network. Fig. 13 illustrates the minimum SNR links in the mesh-based ONoCs using optimized crossbar and Crux optical routers.

As an example, we present the analyses for the minimum SNR link in the mesh-based ONoCs using Crux optical router. On the minimum SNR link, the insertion loss of an optical router $R(i, j)$ at the X-section, $L_{X,i,j}$, and at the Y-section, $L_{Y,i,j}$, for the mesh-based ONoCs using Crux router is calculated in (38) and (39). Regarding (7), the negligible propagation loss inside the routers is not considered ($W_{l_{i,j}} \cong 0$). For simplicity, $L_{i,j}^{OR}$ is shown as $L_{i,j}$. On the right side of these equations, the first subscripts denote the router input ports, and the second subscripts denote the router output ports. Based on these equations, the insertion loss suffered by the minimum SNR link in the mesh-based ONoCs using Crux optical router can be written as (40). In this equation, the seven terms on the right side represent, respectively, the input power, the insertion losses from the source processor to the first optical router, on the X-section of the link, at the optical router where the link turns from the X to Y-section, on the

$$N_{X,j} = \begin{cases} 0, & j = N \\ P_{\text{in}}\left(\frac{L_{\text{in,E}}}{L_c L_b^4 L_{c,\text{off}}^2 L_{p,\text{on}}} k_{p,\text{off}} + L_{\text{in,E}} \frac{L_{W,Ej}}{L_b^2} L_p^D (k_{p,\text{off}} + L_{p,\text{off}}^2 k_c)\right), & j \in [3, N-1] \end{cases} \tag{41}$$

$$N_{Y,i} = \begin{cases} P_{\text{in}}\left(\frac{L_{\text{in,E}}}{L_c L_b^2 L_{c,\text{off}} L_{p,\text{on}}}(k_{p,\text{off}} + L_{p,\text{off}}^2 K_c) + L_{\text{in,E}} L_p^D (k_{p,\text{off}} + L_{p,\text{off}}^2 k_c)\right) \\ +P_{\text{in}}\left(L_{\text{in,E}} \frac{L_{W,Ej}}{L_{p,\text{off}} L_b^2} L_{c,\text{off}} L_{c,\text{on}} L_p^D (k_c + L_c^2 K_{p,\text{off}})\right), & i = 1 \\ P_{\text{in}}\left(\frac{L_{\text{in,E}}}{L_b^2 L_c L_{c,\text{off}} L_{p,\text{on}}}(k_{p,\text{off}} + L_{p,\text{off}}^2 k_c) + L_{\text{in,W}} \frac{L_{E,W}}{L_{p,\text{off}}} L_{c,\text{off}} L_p^D (k_{p,\text{off}} + L_{p,\text{off}}^2 k_c)\right) \\ +P_{\text{in}}\left(L_{\text{in,E}} L_p^D (K_{p,\text{off}} + L_{p,\text{off}}^2 K_c) + L_{\text{in,E}} \frac{L_{W,Ej}}{L_{p,\text{off}}} L_{c,\text{off}}^3 L_p^D K_{p,\text{off}}\right), & i \in [2, M-1] \\ 0, & i = M \end{cases} \tag{42}$$

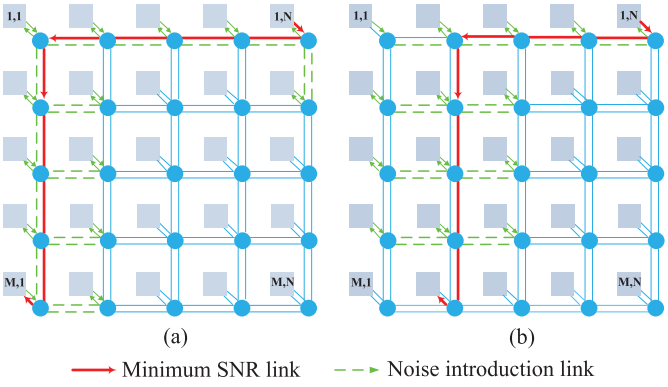

Fig. 13. Minimum SNR link in mesh-based ONoC using (a) optimized crossbar optical router and (b) Crux optical router.

Y-section of the link, at the optical router connected to the destination processor, and the propagation loss. A chip size of 10×10 mm^2 is considered

$$L_{X,i,j} = \begin{cases} L_{\text{in,W}} L_p^D, & i = 1, j = N \\ L_{E,W} L_p^D, & i = 1, 3 \le j \le N-1 \end{cases} \tag{38}$$

$$L_{Y,i,j} = \begin{cases} L_{E,S} L_p^D, & i = 1, j = 2 \\ L_{N,S} L_p^D, & 2 \le i \le M-1, j = 2 \\ L_{N,Ej} L_p^D, & i = M, j = 2. \end{cases} \tag{39}$$

Crosstalk noise will be introduced by the optical signal on the minimum SNR link and optical signals on the other links crossing the minimum SNR link through optical routers. The crosstalk noise introduced at the optical router j on the X-section of the minimum SNR link, N_X, is shown in (41), as shown at the top of the page. The introduced noise at the optical router i on the Y-section of the link, N_Y, is described in (42), as shown at the top of the page. In these equations, P_{in} is the optical input power at the injection port. The total crosstalk noise power can be calculated by summing the crosstalk noise from each Crux router on the link, while the total power loss of the link is given by

$$PL_{SNR_{\text{min,Crux}}} = P_{\text{in}} L_{\text{in,W}} L_{E,W}^{N-3} L_{E,S} L_{N,S}^{M-2} L_{N,Ej} L_p^{D(M+N-3)}. \tag{40}$$

According to (11) and (40)–(42), the minimum SNR of $M \times N$ mesh-based ONoCs is calculated in (41). The mesh-based ONoCs using optimized optical crossbar can be analyzed based on the proposed method and similar to the analyses presented for the mesh-based ONoCs using Crux optical router

$$SNR_{\text{min,Crux}} = 10 \log\left(\frac{PL_{SNR_{\text{min,Crux}}}}{P_{\text{N,Crux}}}\right) \tag{43}$$

$$P_{\text{N,Crux}} = L_{E,S} L_{N,S}^{M-2} L_{N,Ej} L_p^{D(M-1)} \left(\sum_{j=3}^{N-1} L_{E,W}^{j-3} L_p^{D(j-2)} N_{X,3}\right) + L_{N,Ej} L_{N,S}^{M-2} L_p^{D(M-1)} N_{Y,1} + L_{N,Ej} L_p^D \left(\sum_{i=2}^{M-1} L_{N,S}^{M-1-i} L_p^{D(M-1-i)} N_{Y,2}\right).$$

We study the relationship between the network size, the crosstalk noise, and the SNR in the mesh-based ONoCs using the optimized crossbar and Crux optical routers. Numerical simulations are performed using MATLAB. Fig. 14(a) and (b) shows the power of optical signal and crosstalk noise at the destination on the minimum SNR links in the mesh-based ONoCs using optimized crossbar and Crux optical routers, respectively. We find that as the network size increases, the optical signal power received by the destination processor core drops quickly, and the crosstalk noise power increases relatively slow. The reduction in the signal power and the increase in the crosstalk noise power are substantially higher in the mesh-based ONoCs using optimized crossbar. This is due to the large insertion loss of the optimized crossbar, which not only attenuates optical signals but also the crosstalk noise. Using optimized optical crossbar, when the ONoC size is larger than 8×8, the optical signal power is smaller than the crosstalk noise power. For instance, when the network size is 16×16 and P_{in} equals to 0 dBm, the signal power is -24.9 dBm, and the crosstalk noise power is -11 dBm. Comparing with the optimized crossbar, mesh-based ONoCs using Crux router have higher signal power as well as crosstalk noise as indicated in Fig. 14(b). In the mesh-based ONoCs using Crux optical router when the network size is larger than 12×12, the noise power is higher than the signal power. For example, when the network size is 16×16 the

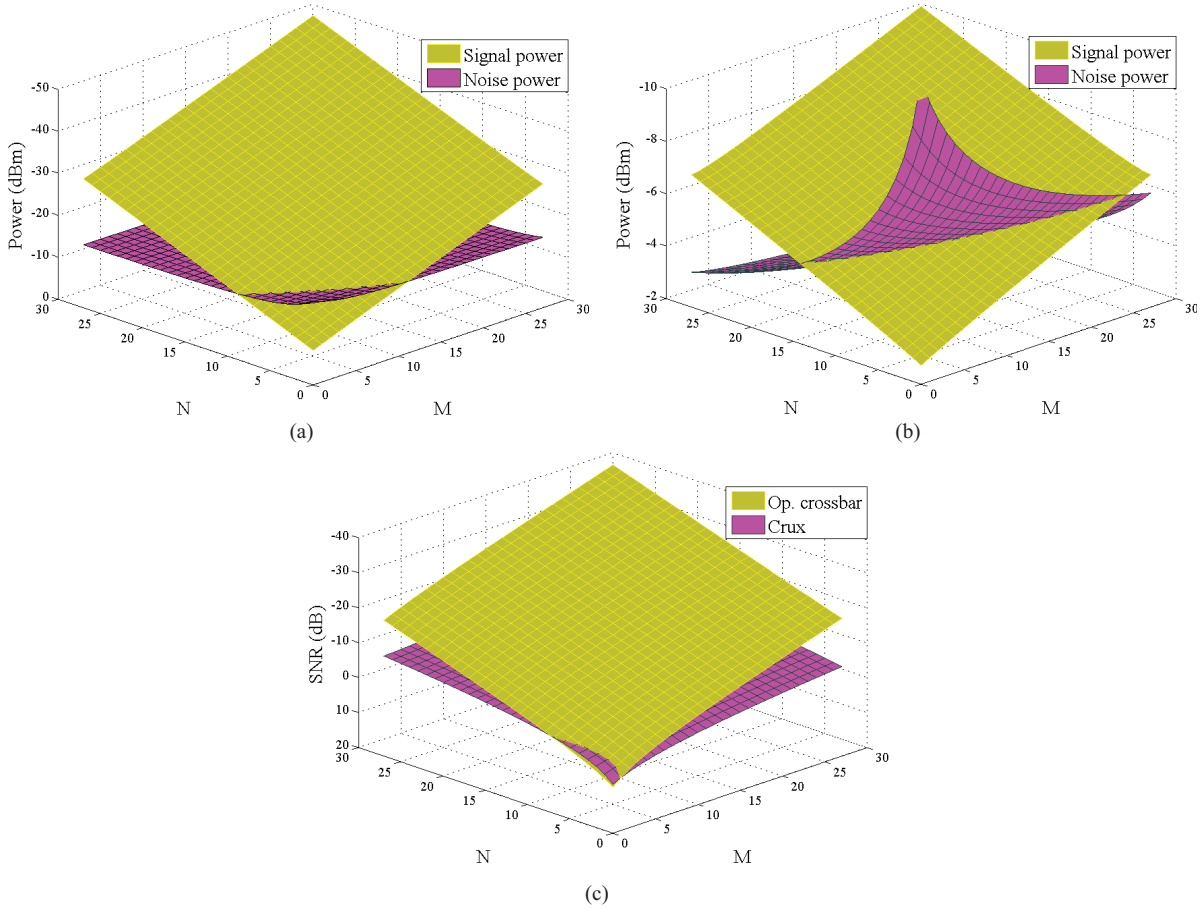

Fig. 14. Signal power, crosstalk noise power, and SNR comparison in $M \times N$ mesh-based ONoCs using the optimized crossbar and Crux optical routers. (a) Optimized optical crossbar router. (b) Crux router. (c) SNR comparison.

signal power and the noise power are -5.9 and -3.6 dBm, respectively.

The minimum SNR comparison in the mesh-based ONoCs using the optimized crossbar and Crux optical routers is shown in Fig. 14(c). This figure shows that as the network size increases, minimum SNR considerably decreases in the mesh-based ONoCs using optimized crossbar while this decline is relatively slow in the mesh-based ONoCs using Crux router. For example, when the network size of the mesh-based ONoC using optimized optical crossbar is 6×6, the minimum SNR is 3.5 dB and when it is 16×16, the minimum SNR will decrease to -13.9 dB, which indicates that the crosstalk noise power is higher than the optical signal power. However, the mesh-based ONoC using Crux has the SNR of 4.8 and -2.4 dB under the same network sizes, respectively. Considering the SNR comparison shown in Fig. 14(c), it can be concluded that the optical router design can highly improve the SNR performance of mesh-based ONoCs.

VI. Conclusion

Crosstalk noise is an intrinsic characteristic of photonic devices used by ONoCs. In large scale ONoCs, crosstalk noise could cause severe performance degradation and prevent ONoCs from communicating properly. For the first time, we presented a systematical formal method to analyze the crosstalk noise and SNR of the optical routers and mesh-based ONoCs. A general 5×5 optical router model was proposed, which can be applied to any other 5×5 optical routers for their crosstalk noise and SNR analyses. The analyses were performed at device, router, and network levels, and were based on the proposed general optical router model. Different longest optical links in the mesh-based ONoCs were analyzed to find the minimum SNR link. We proved that the minimum SNR link in the mesh-based ONoCs should be among the first, the second, and the third longest optical links. We showed that when the network size is equal to a constant number, $M \times N = C$ and C is a constant number, the SNR is the best only when $M = N$. Finally, we used the case studies of the mesh-based ONoCs using the optimized crossbar and Crux optical routers to evaluate the proposed analytical models. We also showed that the SNR performance of the mesh-based ONoCs highly relies on the optical router design. The conclusions drawn in this paper indicate how promising mesh-based ONoCs are among other possible ONoCs architectures.

References

[1] M. Briere, B. Girodias, Y. Bouchebaba, G. Nicolescu, F. Mieyeville, F. Gaffiot, and I. O'Connor, "System level assessment of an optical NoC in an MPSoC platform," in *Proc. Design, Autom. Test Eur. Conf. Exhibit.*, 2007, pp. 1–6.

[2] W. Dally and B. Towles, "Route packets, not wires: On-chip interconnection networks," in *Proc. Design Autom. Conf.*, 2001, pp. 684–689.

[3] *International Technology Roadmap for Semiconductors*. (2010) [Online]. Available: http://www.itrs.net
[4] R. Beausoleil, P. Kuekes, G. Snider, S.-Y. Wang, and R. Williams, "Nanoelectronic and nanophotonic interconnect," *Proc. IEEE*, vol. 96, no. 2, pp. 230–247, Feb. 2008.
[5] F. Xia, L. Sekaric, and Y. Vlasov, "Ultracompact optical buffers on a silicon chip," *Nature Photon.*, vol. 1, pp. 65–71, Dec. 2007.
[6] Y. Xie, M. Nikdast, J. Xu, W. Zhang, Q. Li, X. Wu, Y. Ye, X. Wang, and W. Liu, "Crosstalk noise and bit error rate analysis for optical networkon-chip," in *Proc. ACM/IEEE Design Autom. Conf.*, Jun. 2010, pp. 657–660.
[7] P. Sanchis, J. Galan, A. Brimont, A. Griol, J. Marti, M. Piqueras, and J. Perdigues, "Low-crosstalk in silicon-on-insulator waveguide crossings with optimized-angle," in *Proc. 4th IEEE Int. Conf. Group IV Photon.*, Sep. 2007, pp. 1–3.
[8] W. Bogaerts, P. Dumon, D. V. Thourhout, and R. Baets, "Low-loss, lowcross-talk crossings for silicon-on-insulator nanophotonic waveguides," *Opt. Lett.*, vol. 32, no. 19, pp. 2801–2803, 2007.
[9] H. Chen and A. Poon, "Low-loss multimode-interference-based crossings for silicon wire waveguides," *IEEE Photon. Technol. Lett.*, vol. 18, no. 21, pp. 2260–2262, Nov. 2006.
[10] C.-H. Chen and C.-H. Chiu, "Taper-integrated multimode-interference based waveguide crossing design," *IEEE J. Quantum Electron.*, vol. 46, no. 11, pp. 1656–1661, Nov. 2010.
[11] X. Li, F. Ou, Z. Hou, Y. Huang, and S.-T. Ho, "Experimental demonstration and simulation of lossless metal-free integrated elliptical reflectors for waveguide turnings and crossings," in *Proc. Conf. Lasers Electro-Opt.*, 2011, pp. 1–2.
[12] W. Ding, D. Tang, Y. Liu, L. Chen, and X. Sun, "Compact and low crosstalk waveguide crossing using impedance matched metamaterial," *Appl. Phys. Lett.*, vol. 96, no. 11, pp. 111114–111116, 2010.
[13] J. Chan, G. Hendry, K. Bergman, and L. Carloni, "Physical-layer modeling and system-level design of chip-scale photonic interconnection networks," *IEEE Trans. Comput.-Aided Design Integr. Circuits Syst.*, vol. 30, no. 10, pp. 1507–1520, Oct. 2011.
[14] D. Ding, B. Yu, and D. Z. Pan, "GLOW: A global router for low-power thermal-reliable interconnect synthesis using photonic wavelength multiplexing," in *Proc. Asia South Pacific Design Autom. Conf.*, 2012, pp. 621–626.
[15] M. M. Vaez and C. T. Lea, "Strictly nonblocking directional-coupler-based switching networks under crosstalk constraint," *IEEE Trans. Commun.*, vol. 48, no. 2, pp. 316–323, Feb. 2000.
[16] M. Mohamed, Z. Li, X. Chen, A. Mickelson, and L. Shang, "Modeling and analysis of micro-ring based silicon photonic interconnect for embedded systems," in *Proc. 7th IEEE/ACM/IFIP Int. Conf. Hardw./Softw. Codesign Syst. Synth.*, 2011, pp. 227–236.
[17] P. Dong, W. Qian, S. Liao, H. Liang, C.-C. Kung, N.-N. Feng, R. Shafiiha, J. Fong, D. Feng, A. V. Krishnamoorthy, and M. Asghari, "Low loss silicon waveguides for application of optical interconnects," in *Proc. IEEE Photon. Soc. Summer Topical Meeting Ser.*, Jul. 2010, pp. 191–192.
[18] G.-R. Zhou, X. Li, and N.-N. Feng, "Design of deeply etched antireflective waveguide terminators," *IEEE J. Quantum Electron.*, vol. 39, no. 2, pp. 384–391, Feb. 2003.

Yiyuan Xie received the Ph.D. degree in optical engineering from the Chinese Academy of Science in 2009.

He was a Visiting Scholar with the Hong Kong University of Science and Technology, Hong Kong. He joined the School of Electronic and Information Engineering, Southwest University, Chongqing, China, as a Full Professor, in 2010.

Mahdi Nikdast (S'10) was born in Esfahan, Iran, in 1987. He received the B.Sc. degree in computer engineering (Hons.) from Islamic Azad University, Esfahan, Iran, in 2009. He is currently pursuing the Ph.D. degree with the Department of Electronic and Computer Engineering, Hong Kong University of Science and Technology (HKUST), Hong Kong.

He is currently involved in SNR analyses for ONoCs with the Mobile Computing System Laboratory, HKUST. His research interests include embedded systems, multiprocessor system-on-chip, network-on-chip, and computer architectures.

Mr. Nikdast was a recipient of the Second Best Project Award at the 6th Annual AMD Technical Forum and Exhibition (AMD-TFE 2010).

Jiang Xu (S'02–M'07) received the Ph.D. degree in electrical engineering from Princeton University, Princeton, NJ, in 2007.

He was a Research Associate with Bell Laboratories, NJ, from 2001 to 2002, and with NEC Laboratories America, Princeton, from 2003 to 2005. He joined a startup company, Sandbridge Technologies, Tarrytown, NY, from 2005 to 2007, where he developed and implemented two generations of NoC-based ultralow-power multiprocessor systems-on-chip for mobile platforms. In 2007, he joined the Department of Electronic and Computer Engineering, Hong Kong University of Science and Technology, as an Assistant Professor, and established the Mobile Computing System Laboratory. He has authored or co-authored more than 60 book chapters and papers in peer-reviewed journals and international conferences. His current research interests include network-on-chip, multiprocessor system-on-chip, embedded systems, computer architectures, low-power VLSI design, and HW/SW co-design.

Dr. Xu is currently an Associate Editor of the *ACM Transactions on Embedded Computing Systems* and the IEEE TRANSACTIONS ON VERY LARGE SCALE INTEGRATION SYSTEMS. He is an ACM Distinguished Speaker and a Distinguished Visitor of the IEEE Computer Society. He was on the organizing committees and technical program committees of many international conferences.

Xiaowen Wu, (S'12) photograph and biography are not available at the time of publication.

Wei Zhang, (M'05) photograph and biography are not available at the time of publication.

Yaoyao Ye, (S'09) photograph and biography are not available at the time of publication.

Xuan Wang, (S'12) photograph and biography are not available at the time of publication.

Zhehui Wang, (S'12) photograph and biography are not available at the time of publication.

Weichen Liu, (S'07–M'11) photograph and biography are not available at the time of publication.